

Electron Emission from Individual Indium Arsenide Semiconductor Nanowires

Erwin C. Heeres,[†] Erik P. A. M. Bakkers,[‡] Aarnoud L. Roest,[‡] Monja Kaiser,[‡] Tjerk H. Oosterkamp,[†] and Niels de Jonge^{*,‡,§}

Condensed Matter Physics/Interface Physics, Leiden Institute of Physics, Leiden University, Niels Bohrweg 2, 2333 CA Leiden, The Netherlands, and Philips Research Laboratories, High Tech Campus 4, 5656 AE Eindhoven, The Netherlands

Received October 31, 2006; Revised Manuscript Received January 4, 2007

ABSTRACT

A procedure was developed to mount individual semiconductor indium arsenide nanowires onto tungsten support tips to serve as electron field-emission sources. The electron emission properties of the single nanowires were precisely determined by measuring the emission pattern, current–voltage curve, and the energy spectrum of the emitted electron beam. The two investigated nanowires showed stable, Fowler–Nordheim-like emission behavior and a small energy spread. Their morphology was characterized afterward using transmission electron microscopy. The experimentally derived field enhancement factor corresponded to the one calculated using the basic structural information. The observed emission behavior contrasts the often unstable emission and large energy spread found for semiconductor emitters and supports the concept of Fermi-level pinning in indium arsenide nanowires. Indium arsenide nanowires may thus present a new type of semiconductor electron sources.

Semiconductor nanowires attracted considerable scientific interest on account of the prospect of tunable electronic and optical properties.^{1–3} Nanowires can serve a variety of applications such as single-electron transistors,⁴ sensors in life science,⁵ nanoscale optoelectronic devices,⁶ and tunable superconductors.⁷ Recently, it has been shown that near to ideal ohmic contacts to indium arsenide can be established due to Fermi-level pinning in the conduction band,^{7,8} an effect that is known for bulk indium arsenide.^{9–11} This effect may be used to construct a special type of field-emission electron source from indium arsenide nanowires. Field-emission electron sources made from sharp, semiconductor tips are often difficult to operate in a stable mode because the Fermi level is below the conduction band. When an electric field is applied as needed for field electron emission, insufficient charge carriers are available to maintain a zero potential at the surface, leading to band bending. The resulting emission process is highly unpredictable and exhibits a large energy spread of several tens of electron volts of the emitted electron beam.¹² For this reason, field emitters are usually made from a sharp metal tip¹³ or a tip of a material with metal-like electronic properties, such as a carbon nanotube.¹⁴ Because

of the occurrence of Fermi-level pinning for indium arsenide nanowires, this material could present a special case of a semiconductor electron source with low-energy spread.¹⁵ In this letter, we will describe the construction of the electron source from individual indium arsenide nanowires, demonstrate electron emission, and provide a structural analysis of the emitter.

Single-crystal indium arsenide nanowires grown on an oxidized silicon substrate were produced with an optimized vapor–liquid–solid (VLS) laser ablation method described in detail elsewhere.^{7,16,17} In short, the nanowires were grown on a thermally oxidized silicon substrate, which was covered with an equivalent of a 10 Å gold layer prior to the VLS process. The substrate was heated to approximately 500 °C in order to break up the thin gold film in an argon environment. Indium arsenide was evaporated from a corresponding target using an intense laser beam. The growth mechanism is believed to be the dissolving of indium and arsenic atoms in the locally formed gold droplets until supersaturation and the subsequent growth of the single-crystal nanowires. The growth procedure provided indium arsenide nanowires, with a free electron concentration of about 10^{18} cm^{-3} .⁷ For the investigation of the emission behavior of the material, it is desirable to perform measurements on individually mounted nanowires. Nanowires were first transferred onto a gold-coated silicon substrate with a

* Corresponding author. E-mail: dejongen@ornl.gov.

[†] Leiden University.

[‡] Philips Research Laboratories.

[§] Present address: Oak Ridge National Laboratory, Materials Science and Technology Division, 1 Bethel Valley Road, P.O. Box, 2008, Oak Ridge, Tennessee 37831-6030.

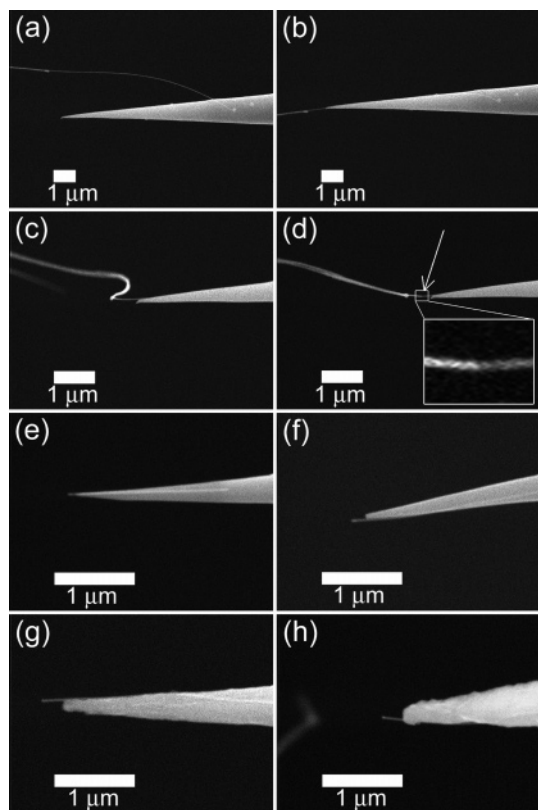


Figure 1. Mounting of an indium arsenide nanowire using nanomanipulators in a scanning electron microscope. (a) Attachment of the protruding nanowire, located on the mounting substrate, to a tungsten support tip. (b) Alignment of the nanowire with respect to the tungsten tip. (c) Bending of the nanowire due to lateral movement. (d) Image of the nanowire after irradiation at the desired break position with the electron beam, showing a contrast difference at this position (inset). (e–h) Four individually mounted nanowires with protruding lengths of 110, 180, 300, and 260 nm, respectively. The nanowires depicted in (g) and (h) are labeled nanowire I and nanowire II and used for the electron emission experiments.

sharp edge (the mounting substrate) in such a way that the nanowires were oriented parallel to the surface and protruding over the edge. The procedure was performed with a micro-manipulator and an optical microscope. Next, a single nanowire was precisely mounted on a sharp tungsten support tip in such way that (1) it was aligned with the central axis through the support tip and (2) only a short length of the nanowire protruded from the support tip. The tungsten tip with a radius of curvature of 50–100 nm was obtained by electrochemical etching of a tungsten wire with a diameter of 0.3 mm that was laser-welded on a heating and support filament made of titanium. The mounting was performed in a scanning electron microscope (SEM), equipped with a nanomanipulator (Omicron),¹⁸ see Figure 1. It is especially important to control the protruding length to minimize vibrations¹⁹ and to prevent excessive Joule heating during field emission.²⁰ The mounting substrate was first searched for a clean, freestanding nanowire with no visible defects and protruding straight from the edge. The selected nanowire was then approached by the tungsten tip and attached to the tungsten tip, see Figure 1a. Prior to the mounting of a nanowire, the support tip was pressed into conductive carbon tape to apply some glue (hydrocarbons) for the attachment

of the nanowire. The nanowire was aligned with the central axis of the tungsten tip by pulling, see Figure 1b. This alignment provided a contact between the nanowire and the tungsten tip, with a typical length of several micrometers. A strong attachment was obtained, and the nanowires could be bent strongly, see Figure 1c. The most difficult step in the mounting procedure was the controlled detachment of the nanowire from the mounting substrate, defining the length of the protruding nanowire. A new method was developed in which the desired break position could be determined within an accuracy of about 100 nm using electron beam irradiation. A mechanically weak position was induced in the nanowires by electron beam irradiation (operating the SEM in spot mode) until a contrast difference occurred on the material (Figure 1d). The current density of the electron beam amounted to $10 \text{ nA}/\mu\text{m}^2$. The nanowire broke at exactly the irradiated position upon applying a mechanical stress by withdrawing the mounting substrate. In Figure 1e–h, four mounted nanowires of different lengths are shown. A total of 10 nanowires with protruding lengths between 110 and 430 nm were mounted. All were tested for electron emission, but some were destroyed by operating them at too-high temperatures or emission current, as was observed by TEM. Others did emit electrons, but a too sharply etched tungsten tip started emitting as well at the typical extraction voltage needed to obtain emission from the nanowires. For two nanowires, all experiments could be completed successfully, as described in the next sections. The mounting procedure could possibly be used for other fields of research as well. For example, to mount nanowires on tips for atomic force microscopy (AFM), similar to what was done for carbon nanotubes.¹⁹ Mounted on an AFM tip, the nanowires could serve as semiconductor probes of a precisely defined symmetry (i.e., nanorod). Additionally, the nanowires could also be functionalized with chemical groups.

The electron emission properties of two individual indium arsenide nanowires were characterized by the following experiments: (1) recording the emission pattern, (2) recording of the current–voltage curve, and (3) recording of the energy spectrum of the emitted electron beam. These experiments were performed in an ultrahigh vacuum chamber with a base pressure of 10^{-10} Torr. Prior to the characterization of the emission properties, each new sample was heated for 2 h at a temperature of approximately 250 °C in order to clean the nanowires from volatile species. The temperature of the support tip was measured with an infrared pyrometer (Iron). The emission pattern was used to check the stability and cleanness of the emitting surface.^{21,22} In Figure 2, two emission patterns of nanowire II are shown. At first, the emission pattern consisted of several spots, which changed their positions with time, indicating a lack of stability or cleanness of the surface. By slowly increasing the emission current, the nature of the emission pattern changed with time. The maximal current was kept below 0.5 nA because it was found that currents well above 10 nA led to a damaged structure, possibly due to Joule heating. A single stable bright spot in the emission pattern was finally obtained after running the emitter for 30 min. Similar results were obtained for

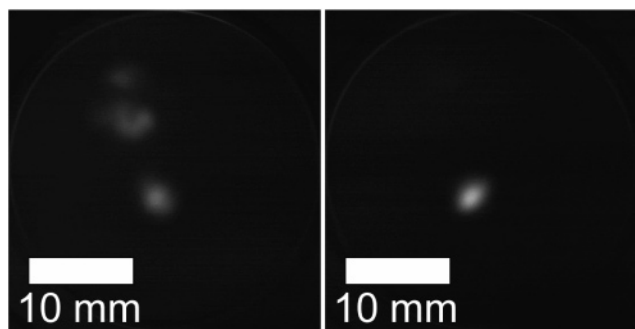


Figure 2. Emission patterns of nanowire II after heat treatment recorded with a microchannel plate and a phosphor screen. (left) Emission pattern recorded directly after starting the emission with an extraction voltage of 444 V and 100 pA of emission current. (right) Emission pattern recorded after 30 min of emission for 449 V and 320 pA.

nanowire I (data not shown). As has been observed previously for carbon nanotubes,^{21,22} the fluctuating emission pattern could originate from species being adsorbed at the apex of the emitter and a consecutive change of the work function at that location. By Joule heating of the wire, during emission, the adsorbed impurities were evaporated from the emitter, leading to stable emission. Another possibility is a slight reshaping of the emission site, i.e., the nanowire apex, leading to an equilibrium indium arsenide structure under the influence of the strong electric field and Joule heating. Depending on the temperature and the field, the reshaping can either be dulling or sharpening of the tip. Dulling is often found for metallic electron sources and leads to a more homogeneous emission pattern.^{23,24} Sharpening often leads to less emission stability, although special states in which a small tip on top of the main tip, a so-called supertip is formed, which may present a new stable configuration with a narrow emission beam.²⁵

The electron emission process was further characterized by measuring the current–voltage curves of the two emitters, see Figure 3a and b. Current–voltage curves were recorded with a source meter (Keithley) and software of local design in LabView (National Instruments). Because of the Fermi-level pinning effect, we expect that the electron emission can be described by the Fowler–Nordheim field-emission model.^{26,27} The tunneling current density J through a potential barrier between a metal surface and vacuum in a modified equation of the Fowler–Nordheim model is given by:^{14,28}

$$J = c_1 \frac{F^2}{b_1^2 \phi} \exp \left\{ a_2 c_2 c_3^2 \frac{1}{\sqrt{\phi}} \right\} \exp \left\{ -a_1 c_2 \frac{\phi^{3/2}}{F} \right\} \quad (1)$$

with work function ϕ , electric field F , and the constants $a_1 = 0.958$, $a_2 = 1.05$, $b_1 = 1.05$, $c_1 = e^3/8\pi h$, $c_2 = 8\pi\sqrt{(2m_e)}/3he$, $c_3 = e^3/4\epsilon_0$, with the electron mass m_e , Planck's constant h , the electron charge e , and permittivity of free space ϵ_0 . Assuming a hemispherical shape of the emitting surface with radius R , a total emitted current of $I = 2\pi R^2 J$ is obtained. The sharp curvature of the emitting surface leads to field enhancement by a field factor β , $F = \beta U$, where U is the

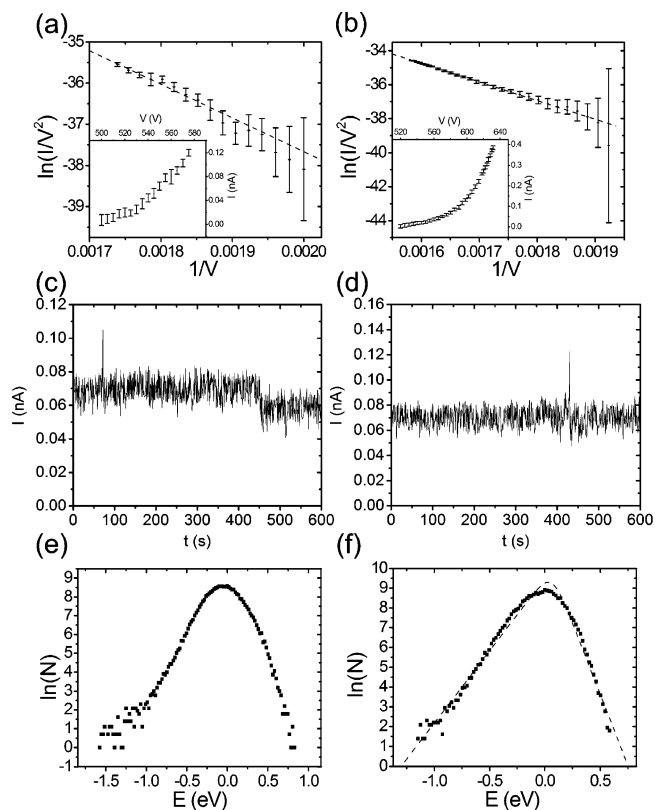


Figure 3. Characterization of the electron emission process of nanowire I (a,c,e) and II (b,d,f). In (a) and (b), the current–voltage characteristics are given in the form of the Fowler–Nordheim plot. The dashed lines represent fitting of the Fowler–Nordheim model to the data. The insets show the measured current–voltage curves. Plots of the emission current as a function of time are shown in (c) and (d). The extraction voltage is kept constant at 553 and 582 V, respectively. Images (e) and (f) show the energy spectra of the emitted electron beam recorded at currents of 70 pA and 185 pA, respectively.

Table 1. Results of the Electron Emission Measurements and the TEM Imaging on Nanowires I and II^a

wire	R_{fit} (nm)	β_{fit} ($\times 10^6 \text{ m}^{-1}$)	L_{TEM} (nm)	R_{TEM} (nm)	$\beta_{\text{numerical}}$ ($\times 10^6 \text{ m}^{-1}$)
I	0.2 ± 0.1	8.7 ± 0.7	300	11	8.2
II	2.1 ± 0.4	6.5 ± 0.2	270	10	7.9

^a R_{fit} is the radius of the nanowire obtained by fitting the Fowler–Nordheim model to the data. β_{fit} is the corresponding field enhancement factor. L_{TEM} is the length of the fraction of the nanowire protruding from the support tip, as determined from the TEM image, and R_{TEM} is the related radius. $\beta_{\text{numerical}}$ is the numerically calculated field enhancement factor using the radius and length from the TEM image.

potential difference between anode and cathode. It thus follows that $\log(I/U^2)$ is proportional to $1/U$, a plot of which is called a Fowler–Nordheim curve (see Figure 3a and b). Table 1 gives the values of the field enhancement factor β_{fit} and the radius of the emitting area R_{fit} , as obtained by fitting the data to the Fowler–Nordheim model and assuming $\phi = 4.9 \text{ eV}$.²⁹ A linear relation in the measured current regime of up to 120 pA for nanowire I and 400 pA for nanowire II can be observed, indicating that a field-emission mechanism occurs. Fowler–Nordheim behavior was previously found for tips made of macroscopic samples of indium arsenide.³⁰

Because both nanowires emitted currents that were equal within a factor of 2 for the same voltage, it can also be concluded that both nanowires had similar properties and shapes.

To show the stability of the emission process, the emitted current was recorded at constant extraction voltage as a function of time, see Figure 3c and d. Over a time period of 10 min, the measured current fluctuations are about 0.01 nA, close to the noise floor of our measurement system, with occasional spikes of the current.

A third important aspect of the emission process is the energy spectrum of the emitted electron beam. For a field emitter, the current density as a function of energy E is given by the equation:²⁷

$$J(E) \propto \frac{\exp(E/d)}{1 + \exp(E/k_B T)} \quad (2)$$

with k_B the Boltzmann constant, T the temperature, and d the tunneling parameter. Energy spectra were recorded for both nanowires (Figure 3e and f) with a hemispherical energy analyzer with a resolution of 50 meV (VSW). An energy spectrum was recorded shortly after the recording of the current–voltage curve and without changing the position of the nanowire. The widths of the spectra were determined by calculating the full width at half-maximum (fwhm) and subtracting 50 meV to compensate for the broadening of the spectrum analyzer.¹⁴ The beams coming from nanowires I and II had energy widths ΔE of 0.40 and 0.33 eV, respectively. These values are much smaller than the energy widths of emitters from silicon tips, which can amount to up to several tens of eV.¹² The energy widths are comparable to the values of tungsten field emitters,²³ with $\Delta E = 0.3$ eV, and carbon nanotube emitters,¹⁴ with $\Delta E = 0.35$ eV (typically measured at currents of between 1 and 100 nA). This observation supports the conclusion that the nanowires exhibit field-emission-like behavior, as expected on account of the effect of Fermi-level pinning. It should be noted that the performance of semiconductor emitters can sometimes be enhanced by heavy doping. In the case of nanometer-sized structures, however, the controlled doping level presents a serious problem due to the very small total number of doping atoms in the nanostructure for typical doping levels used in bulk materials.³⁰

For a detailed understanding of the emission characteristics of any material, it is required to investigate the relation between the emission properties and the structure of the material. We have imaged both nanowires with a Tecnai F30ST transmission electron microscope (TEM, FEI Company) after the emission experiments. To avoid electron-beam-induced damage of the nanowire, objective astigmatism and focus were adjusted on a position near and not on the nanowire. The images for nanowire I are shown in Figure 4. The high-resolution TEM images reveal the crystal planes perpendicular to the longitudinal direction of the nanowire. A lattice spacing of 3.50 ± 0.04 Å was determined, corresponding well to the $\langle 111 \rangle$ plane spacing of indium arsenide of 3.4980 Å.^{31,32} The lattice constant for indium

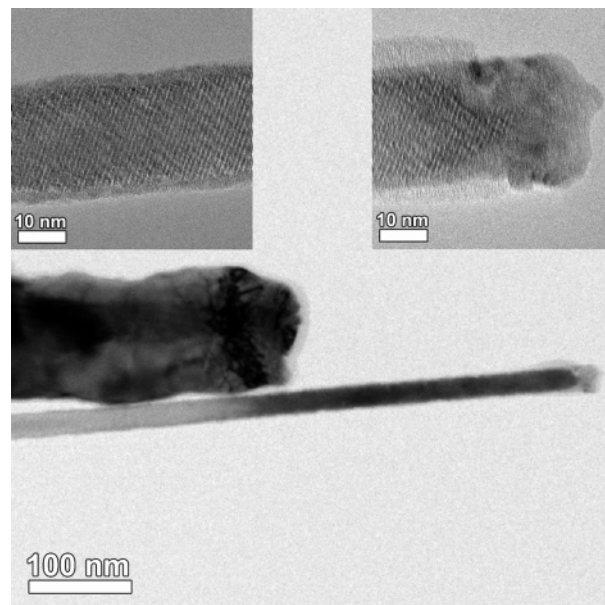


Figure 4. Transmission electron microscope (TEM) image of nanowire I on a tungsten support tip. (left inset) High-resolution TEM image of the middle part of the wire in which the crystal planes are resolved. The longitudinal direction of the wire is $\langle 111 \rangle$. (right inset) High-resolution TEM image of the apex of the nanowire showing a polycrystalline fraction.

arsenide $a_0 = 0.60584$ nm. Therefore, the distance between the $\langle 111 \rangle$ crystal planes is $a_0/\sqrt{3} = 0.34980$ nm. The TEM images also show a thin amorphous layer surrounding the wire over its entire length and amorphous material with a thickness of about 20 nm at the apex.

The length L_{TEM} and radius R_{TEM} were determined from the TEM image to respective values of 300 and 11 nm. These values were used to calculate the field enhancement factor. Numeric calculations of the electric field were performed with the program EMECH (Munro's Electron Beam Software). A rod on a support tip with the same dimensions as determined from the TEM images was modeled in 3D, assuming axial symmetry. The field enhancement factor was calculated to amount to $\beta_{\text{numerical}} = 8.2 \times 10^6 \text{ m}^{-1}$. The same analysis was performed for the other nanowire. Table 1 compares the obtained values R_{TEM} and $\beta_{\text{numerical}}$, with the values determined from the emission measurements R_{fit} and β_{fit} . For both nanowires, the values of the field enhancement factor agreed within about 20%. This implies that it is reasonable to apply the Fowler–Nordheim model. It also indicates that the shape as seen by the electric field, determining the experimentally obtained field enhancement factor, is approximately equal to the actual shape as determined with TEM. The values of the radii as obtained from the emission experiment are much smaller than the wire radii as obtained from the TEM images. The radius as determined from the fit of the current–voltage curve is mainly determined by the size of the emitting area. Looking at Figure 4, however, a sharp protrusion is visible at the apex of the nanowire, with a radius of curvature of about 2 nm. This protrusion might have provided an additional field enhancement, which could have led to a preference of the emission to occur from the protrusion (compare, e.g., the

supertip emitter²⁵), while the total field enhancement given by the high-aspect nanowires and the support tip hardly changes.

Energy dispersive X-ray (EDX) spectra were recorded to investigate the chemical contents of the nanowires. Spectra were obtained at various positions at the nanowires. From the data obtained at the middle, an In/As ratio of 45:55 ($\pm 10\%$) was determined. This agrees within the experimental error with the expected stoichiometry of 1:1. EDX data obtained at the apex shows the presence of indium and arsenic in a 60:40 ($\pm 10\%$) ratio. This differs slightly from the ratio obtained at the bulk wire, which could indicate that some As has been removed from the wire's apex. The transformation of the single-crystalline wire's apex into amorphous material can be caused by heating, or electron beam damage in the breaking procedure during mounting, or due to the influence of Joule heating and the electric field during the emission experiments.^{20,32} In the bulk of the nanowire, the mean free path for the electrons is 10–100 nm.⁷ We do not know whether the mean free path in the apex is considerably smaller. If it is much smaller than the dimensions of the amorphous cap, it might influence the emission properties if the scattering is predominantly inelastic. If it is of the same size as the cap, the influence of the cap on the emission properties is expected to be small.

In summary, a precise procedure was developed to mount individual indium arsenide nanowires on sharp tungsten support tips. This procedure could possibly find general application for the construction of nanowire probes for, e.g., atomic force microscopy. A detailed investigation of the electron emission properties of individual indium arsenide nanowires was performed. The emission exhibited a narrow electron beam, Fowler–Nordheim-like emission behavior, and a small energy spread. This emission behavior contrasts unstable emission and large energy spread as found for semiconductor emitters and supports the concept of Fermi-level pinning in indium arsenide nanowires. The indium arsenide nanowire thus presents a special type of electron source. The field enhancement factors as determined by fitting the emission data corresponded to the value calculated using the structural information from the TEM images. We envision that indium arsenide nanowire emitters may show emission occurring from quantum confined states when the emitters are externally cooled.

Acknowledgment. We thank T. van Rooij for experimental help. This work was supported by FEI Company and the Dutch Ministry of Economic Affairs.

References

- (1) Yang, P. *MRS Bull.* **2005**, *30*, 85–91.

- (2) Xia, Y.; Yang, P.; Sun, Y.; Wu, Y.; Mayers, B.; Gates, B.; Yin, Y.; Kim, F.; Yan, H. *Adv. Mater.* **2003**, *15*, 353–389.
- (3) Lieber, C. M. *MRS Bull.* **2003**, *28*, 486–491.
- (4) De Franceschi, S.; van Dam, J. A.; Bakkers, E. P. A. M.; Feiner, L. F.; Gurevich, L.; Kouwenhoven, L. P. *Appl. Phys. Lett.* **2003**, *83*, 344–346.
- (5) Patolsky, F.; Zheng, G.; Lieber, C. M. *Nanomedicine* **2006**, *1*, 51–65.
- (6) Duan, X.; Huang, Y.; Cui, Y.; Wang, J.; Lieber, C. M. *Nature* **2001**, *409*, 66–69.
- (7) Doh, Y.-J.; van Dam, J. A.; Roest, A. L.; Bakkers, E. P. A. M.; Kouwenhoven, L. P.; De Franceschi, S. *Science* **2005**, *309*, 272–275.
- (8) Wildoer, J. W. G.; Harmans, C. J. P. M.; van Kempen, H. *Phys. Rev. B* **1997**, *55*, 16013–16016.
- (9) Sze, S. M. *Physics of Semiconductor Devices*; John Wiley & Sons: New York, 1981.
- (10) van Wees, B. *Phys. World* **1996**, *9*, 41–45.
- (11) Mohan, P.; Motohisa, J.; Fukui, T. *Appl. Phys. Lett.* **1996**, *88*, 13110.
- (12) Zhu, W.; Zhu, W. *Vacuum Microelectronics*; John Wiley & Sons: New York, 2002.
- (13) Good, R. H.; Mueller, E. W. Field Emission. In *Handbuch der Physik*, XXI, Fluegge, S., Ed.; Springer-Verlag: Berlin, 1956; Vol. 21, pp 176–231.
- (14) de Jonge, N.; Allieux, M.; Oostveen, J. T.; Teo, K. B. K.; Milne, W. I. *Phys. Rev. Lett.* **2005**, *94*, 186807-1–4.
- (15) de Jonge, N.; Bakkers, E. P. A. M.; Feiner, L. F.; Calvosa, A. M. Electron source with low energy spread. European Patent EP 1 641 012, 2005.
- (16) Morales, A. M.; Lieber, C. M. *Science* **1998**, *279*, 208–211.
- (17) Bakkers, E. P. A. M.; van Dam, J. A.; De Franceschi, S.; Kouwenhoven, L. P.; Kaiser, M.; Verheijen, M.; Wondergem, H.; Van der Sluis, P. *Nat. Mater.* **2004**, *3*, 769–773.
- (18) de Jonge, N.; Lamy, Y.; Kaiser, M. *Nano Lett.* **2003**, *3*, 1621–1624.
- (19) Hafner, J. H.; Cheung, C.-L.; Oosterkamp, T. H.; Lieber, C. M. *J. Phys. Chem. B* **2001**, *105*, 743–746.
- (20) Purcell, S. T.; Vincent, P.; Journet, C.; Binh, V. T. *Phys. Rev. Lett.* **2002**, *88*, 105502-1–4.
- (21) de Jonge, N.; Doytcheva, M.; Allieux, M.; Kaiser, M.; Mentink, S. A. M.; Teo, K. B. K.; Lacerda, R. G.; Milne, W. I. *Adv. Mater.* **2005**, *17*, 451–455.
- (22) Dean, K. A.; Chalamala, B. R. *J. Vac. Sci. Technol., B* **2003**, *21*, 868–871.
- (23) Charbonnier, F. *Appl. Surf. Sci.* **1996**, *94–95*, 26–43.
- (24) Swanson, L. W.; Schwind, G. A. A Review of the Zr/O Schottky Cathode. In *Handbook of Charged Particle Optics*; Orloff, J., Ed.; CRC Press: New York, 1997; pp 77–102.
- (25) Kalbitzer, S.; Knoblauch, A. *Rev. Sci. Instrum.* **1998**, *69*, 1026–1031.
- (26) Fowler, R. H.; Nordheim, L. W. *Proc. R. Soc. London, Ser. A* **1928**, *119*, 173–181.
- (27) Hawkes, P. W.; Kasper, E. *Principles of Electron Optics*; Academic Press: London, 1989.
- (28) Groening, O.; Kuettel, O. M.; Emmenegger, C.; Groening, P.; Schlapbach, L. *J. Vac. Sci. Technol., B* **2000**, *18*, 665–678.
- (29) Gobeli, G. W.; Allen, F. G. *Phys. Rev.* **1965**, *137*, A245–A254.
- (30) Truxillo, S. G.; Blair, J. C.; Einspruch, N. G.; Stratton, R. J. *Chem. Phys.* **1966**, *44*, 1724–1725.
- (31) Giesecke, G.; Pfister, H. *Acta Crystallogr.* **1958**, *11*, 369–371.
- (32) Fursey, G. *Appl. Surf. Sci.* **1996**, *94–95*, 44–59.

NL062554R